

# Evidence for the aldo-keto reductase pathway of polycyclic aromatic *trans*-dihydrodiol activation in human lung A549 cells

Jong-Heum Park\*, Dipti Mangal†, Kirk A. Tacka\*, Amy M. Quinn\*, Ronald G. Harvey‡, Ian A. Blair\*†, and Trevor M. Penning\*†§

\*Center of Excellence in Environmental Toxicology and †Center for Cancer Pharmacology, Department of Pharmacology, University of Pennsylvania School of Medicine, Philadelphia, PA 19104-6084; and ‡The Ben May Institute for Cancer Research, University of Chicago, Chicago, IL 60637

Communicated by William F. DeGrado, University of Pennsylvania School of Medicine, Philadelphia, PA, March 20, 2008 (received for review October 30, 2007)

Polycyclic aromatic hydrocarbons (PAHs) are tobacco carcinogens implicated in the causation of human lung cancer. Metabolic activation is a key prerequisite for PAHs to cause their deleterious effects. Using human lung adenocarcinoma (A549) cells, we provide evidence for the metabolic activation of ( $\pm$ )-*trans*-7,8-dihydroxy-7,8-dihydrobenzo[*a*]pyrene (B[*a*]P-7,8-*trans*-dihydrodiol) by aldo-keto reductases (AKRs) to yield benzo[*a*]pyrene-7,8-dione (B[*a*]P-7,8-dione), a redox-active *o*-quinone. We show that B[*a*]P-7,8-*trans*-dihydrodiol (AKR substrate) and B[*a*]P-7,8-dione (AKR product) lead to the production of intracellular reactive oxygen species (ROS) (measured as an increase in dichlorofluorescein diacetate fluorescence) and that similar changes were not observed with the regioisomer ( $\pm$ )-*trans*-4,5-dihydroxy-4,5-dihydrobenzo[*a*]pyrene or the diol-epoxide, ( $\pm$ )-*anti*-7,8-dihydroxy-9 $\alpha$ ,10 $\beta$ -epoxy-7,8,9,10-tetrahydro-B[*a*]P. B[*a*]P-7,8-*trans*-dihydrodiol and B[*a*]P-7,8-dione also caused a decrease in glutathione levels and an increase in NADP<sup>+</sup>/NADPH ratios, with a concomitant increase in single-strand breaks (as measured by the comet assay) and 7,8-dihydro-8-oxo-2'-deoxyguanosine (8-oxo-dGuo). The specificity of the comet assay was validated by coupling it to human 8-oxo-guanine glycosylase (hOGG1), which excises 8-oxo-Gua to yield single-strand breaks. The levels of 8-oxo-dGuo observed were confirmed by an immunoaffinity purification stable isotope dilution ([<sup>15</sup>N<sub>5</sub>]-8-oxo-dGuo) liquid chromatography-electrospray ionization/multiple reaction monitoring/mass spectrometry (LC-ESI/MS) assay. B[*a*]P-7,8-*trans*-dihydrodiol produced DNA strand breaks in the hOGG1-coupled comet assay as well as 8-oxo-dGuo (as measured by LC-ESI/MS) and was enhanced by a catechol *O*-methyl transferase (COMT) inhibitor, suggesting that COMT protects against *o*-quinone-mediated redox cycling. We conclude that activation of PAH-*trans*-dihydrodiols by AKRs in lung cells leads to ROS-mediated genotoxicity and contributes to lung carcinogenesis.

8-oxo-dGuo | DNA strand breaks | tobacco carcinogens | reactive oxygen species

Polycyclic aromatic hydrocarbons (PAHs) are ubiquitous environmental pollutants, which are produced as a result of fossil-fuel combustion and are found in car exhaust and char-broiled and smoked foods (1, 2). They are also present as mixtures in tobacco smoke and are implicated in the causation of human lung cancer (3). To exert their carcinogenic effects, PAHs must be metabolically activated to DNA-damaging agents that will result in the signature mutations in lung cancer. These mutations are G-to-T transversions that either activate the *K-ras* protooncogene at the 12th and 61st codon (4) or inactivate the *p53* tumor suppressor gene at hot spots in its DNA binding domain (5).

Using benzo[*a*]pyrene (B[*a*]P) as a representative PAH, three pathways of activation have been proposed that lead to these mutations. The first pathway involves the formation of (+)-*anti*-7 $\alpha$ ,8 $\beta$ -dihydroxy-9 $\alpha$ ,10 $\beta$ -epoxy-7,8,9,10-tetrahydroB[*a*]P {( $\pm$ )-

*anti*-B[*a*]PDE}. In this pathway there is sequential monooxygenation catalyzed by cytochrome P450 (P450) 1A1/1B1 and hydration to form 7 $\alpha$ ,8 $\beta$ -dihydroxy-7,8-dihydroxy-B[*a*]P, which undergoes a secondary monooxygenation to form (+)-*anti*-B[*a*]PDE (6). This diol-epoxide forms stable (+)-*anti*-*trans*-B[*a*]PDE-N<sup>2</sup>-2'-deoxyguanosine (dGuo) adducts, which via *trans*-lesional bypass DNA polymerases, yield G-to-T transversions (7).

The second pathway involves metabolic activation by P450 peroxidases to yield radical cations (8), which can form depurinating adducts that lead to abasic sites. Apurinic/aprimidinic (AP) sites, if not repaired, can give rise to G-to-T transversions (9). However, it is unlikely that radical cations are sufficiently long-lived to damage DNA in intact cells.

The third pathway of PAH activation is the NAD(P<sup>+</sup>)-dependent oxidation of PAH-*trans*-dihydrodiols to PAH *o*-quinones catalyzed by dihydrodiol dehydrogenase members of the aldo-keto reductase (AKR) superfamily (10). AKRs divert PAH *trans*-dihydrodiols to form ketols that spontaneously rearrange to catechols (Scheme 1). The catechols undergo two one-electron oxidation events to produce the corresponding redox-active and electrophilic *o*-quinones. PAH *o*-quinones can form stable and depurinating DNA adducts *in vitro* (11, 12), and these adducts may provide a route to G-to-T transversion mutations.

In the presence of NAD(P)H, PAH *o*-quinones also undergo nonenzymatic reduction back to catechols. This event establishes futile redox cycles, which amplify the generation of reactive oxygen species (ROS) at the expense of NADPH and may lead to a prooxidant cellular state. Because a prooxidant state has been associated with tumor initiation and promotion (13), the AKR pathway of PAH activation is attractive in that it could explain how PAHs act as complete carcinogens. In addition, ROS may cause oxidative DNA damage such as 7,8-dihydro-8-oxo-2'-deoxyguanosine (8-oxo-dGuo) lesions, which can lead to G-to-T transversions (14). Amplification of ROS by catechol-*o*-quinone interconversion has also been proposed as a cause of estrogen carcinogenesis (15).

Using a yeast gap repair assay to detect *p53* mutations, Yu *et al.* (16) showed that PAH *o*-quinones were more potent as mutagens than ( $\pm$ )-*anti*-7,8-dihydroxy-9 $\alpha$ ,10 $\beta$ -epoxy-7,8,9,10-tetrahydroB[*a*]P (*anti*-B[*a*]PDE) provided that the *o*-quinones were allowed to redox cycle. Furthermore, the mutation pattern

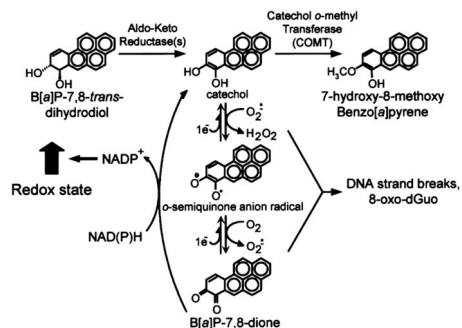
Author contributions: J.-H.P. and T.M.P. designed research; J.-H.P., D.M., K.A.T., and A.M.Q. performed research; R.G.H. and I.A.B. contributed new reagents/analytic tools; J.-H.P., D.M., K.A.T., and A.M.Q. analyzed data; and J.-H.P. and T.M.P. wrote the paper.

The authors declare no conflict of interest.

§To whom correspondence should be addressed. E-mail: penning@pharm.med.upenn.edu.

This article contains supporting information online at [www.pnas.org/cgi/content/full/0802776105/DCSupplemental](http://www.pnas.org/cgi/content/full/0802776105/DCSupplemental).

© 2008 by The National Academy of Sciences of the USA



**Scheme 1.** Metabolic activation of B[a]P-7,8-*trans*-dihydrodiol by AKRs and ROS formation.

observed was dominated by G-to-T transversions. These mutations were suppressed by ROS attenuators. Recent HPLC-electrochemical detection (ECD) analysis showed that there was a direct linear correlation between 8-oxo-dGuo formation and mutagenic frequency in *p53* observed with PAH *o*-quinones (17).

Five human AKR isoforms including aldehyde reductase (AKR1A1) and hydroxysteroid dehydrogenases AKR1C1–AKR1C4 have been implicated in PAH activation (10). Jiang *et al.* (18, 19) showed that ( $\pm$ )-*trans*-7,8-dihydroxy-7,8-dihydro B[a]P (B[a]P-7,8-*trans*-dihydrodiol) is activated to the corresponding B[a]P-7,8-dione in H358 human lung bronchoalveolar cell lysates and intact cells stably transfected with AKR1A1. Palackal *et al.* (20) also demonstrated that 7,12-dimethylbenz[a]anthracene-3,4-dihydrodiol is activated to 7,12-dimethylbenz[a]anthracene-3,4-dione in A549 lung adenocarcinoma cell extracts that constitutively overexpress AKR1C1–AKR1C3 isoforms. Clinical and epidemiological studies have suggested that AKR expression is positively correlated with the development of lung cancer. AKRs are up-regulated in nonsmall cell lung carcinoma (NSCLC) and

the bronchial epithelium of smokers (21). AKR1C1 and AKR1B10 were also two of seven genes among 30,000 genes most overexpressed in smokers with NSCLC (22). However, despite this evidence, the hypothesis that PAH activation by AKRs results in ROS amplification, a prooxidant state, and oxidative DNA damage has not yet been formally tested in human lung cells.

We show that B[a]P-7,8-*trans*-dihydrodiol (AKR substrate) and B[a]P-7,8-dione (AKR product) generate ROS and create a prooxidant cellular state (i.e., change in cellular redox status) in A549 lung adenocarcinoma cells. We also show that conversion of B[a]P-7,8-*trans*-dihydrodiol to B[a]P-7,8-dione by the AKR pathway causes DNA strand breaks and 8-oxo-dGuo formation. These findings support a role for the AKR pathway in human lung carcinogenesis.

## Results

**Metabolic Activation of B[a]P-7,8-*trans*-Dihydrodiol to B[a]P-7,8-Dione in A549 Cells.** To determine whether AKR1C isoforms could convert B[a]P-7,8-*trans*-dihydrodiol to B[a]P-7,8-dione, A549 cell extracts and intact cells were incubated with 10  $\mu$ M [ $^3$ H]-B[a]P-7,8-*trans*-dihydrodiol in the presence of NADP<sup>+</sup> or unlabeled 10  $\mu$ M B[a]P-7,8-*trans*-dihydrodiol, respectively. The reactions in cell extracts and intact cells were monitored by HPLC-UV/ $\beta$ -radioactivity monitor and liquid chromatography-electrospray ionization/mass spectrometry (LC-ESI/MS), respectively.

In the A549 cell extracts B[a]P-7,8-*trans*-dihydrodiol was converted to B[a]P-7,8-dione, which was trapped with  $\beta$ -mercaptoethanol *in situ* as a thio-ether conjugate. The conjugate was identified by coelution with an authentic synthetic standard that was characterized by LC-atmospheric pressure chemical ionization (APCI)/MS, as described (Fig. 1 *A* and *C*) (18, 19). The formation of B[a]P-7,8-dione was maximal at the earliest time point taken (2 h) at which point only 15% of the B[a]P-7,8-*trans*-dihydrodiol was metabolized (Fig. 1 *A* and *B*).

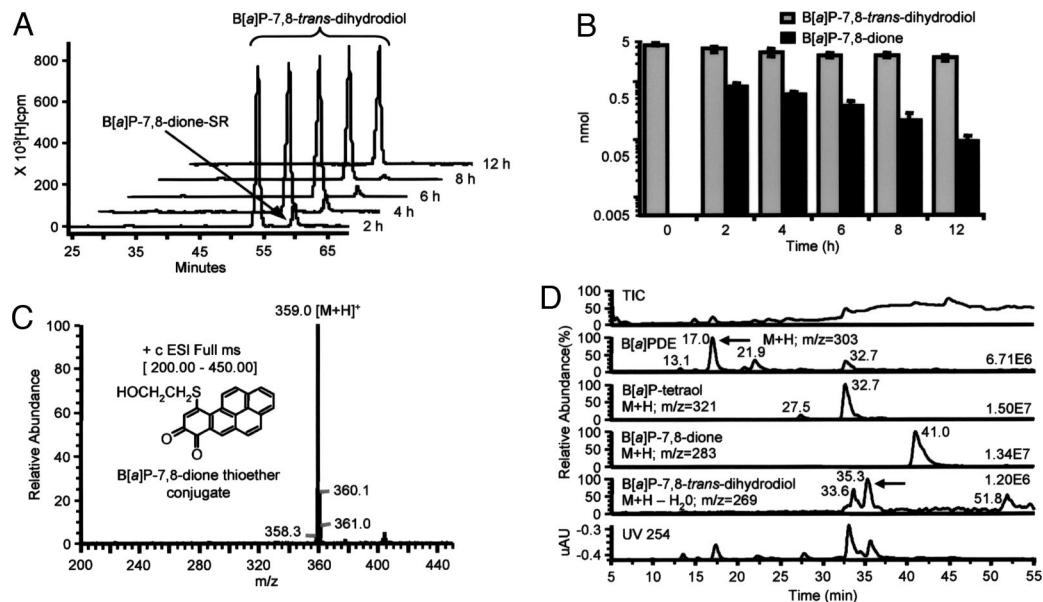


**Fig. 1.** Metabolic activation of B[a]P-7,8-*trans*-dihydrodiol to B[a]P-7,8-dione by AKR1C isoforms in A549 cells. (*A*) [ $^3$ H]-B[a]P-7,8-*trans*-dihydrodiol consumption and B[a]P-7,8-dione formation in A549 cell extracts. (*B*) Changes in the relative amounts (in nmol) of B[a]P-7,8-*trans*-dihydrodiol and B[a]P-7,8-dione over 12 h in cell extracts. Mean  $\pm$  SD ( $n = 3$ ) is shown. (*C*) APCI-positive ion mass spectral identification of B[a]P-7,8-dione thioether conjugate obtained by using a Finnigan TSQ Quantum Ultra AM. MRM for B[a]P-7,8-dione-thioether conjugate detected the following ion transition:  $m/z = 359$  [M+H]<sup>+</sup>. (*D*) LC-MS/MRM chromatograms of organic soluble extracts from intact cells after treatment with B[a]P-7,8-*trans*-dihydrodiol for 12 h. TIC, total ion current; B[a]PDE, Rt 17.0 min,  $m/z = 303$  [M+H]<sup>+</sup>; B[a]P-tetraols, Rt 27.5 and 32.7 min,  $m/z = 321$  [M+H]<sup>+</sup>; B[a]P-7,8-dione, 41.0 min,  $m/z = 283$  [M+H]<sup>+</sup>; B[a]P-7,8-*trans*-dihydrodiol, 35.0 min,  $m/z = 269$  [M+H - H<sub>2</sub>O]<sup>+</sup>; uAU, absorbance units at 254 nm.

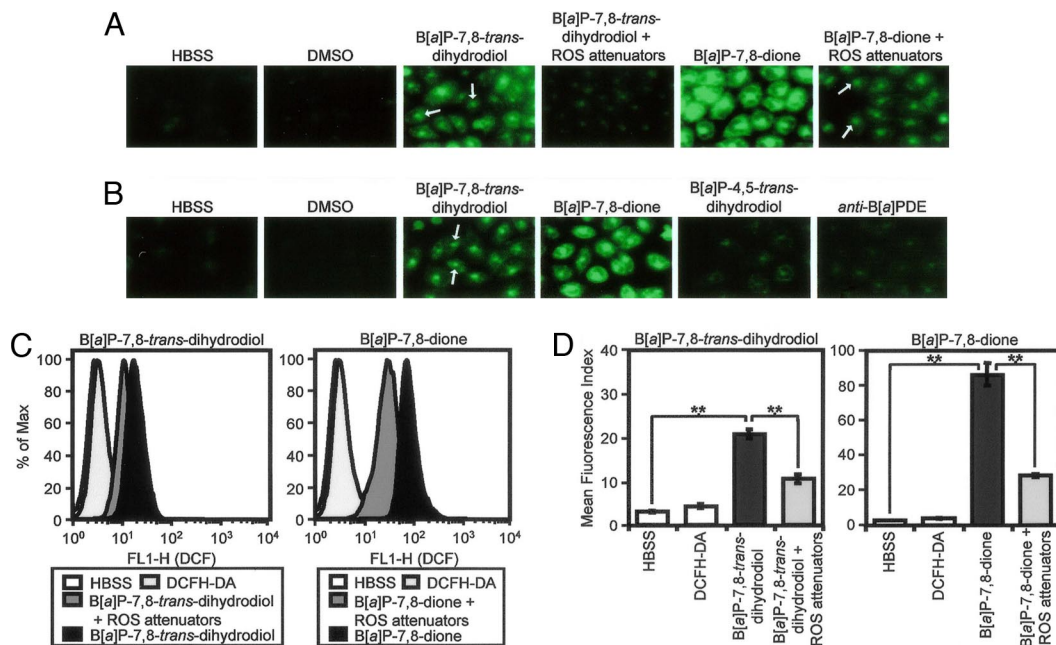


**Fig. 2.** DCFH-DA detection of ROS in A549 cells-treated with PAH metabolites. (A) ROS formation in A549 cells-mediated by B[a]P-7,8-*trans*-dihydrodiol and B[a]P-7,8-dione. DCFH-DA-pretreated A549 cells were incubated with 20  $\mu$ M B[a]P metabolites in the absence and presence of desferal (1 mM) and  $\alpha$ -tocopherol (250  $\mu$ M) for 6 h at 37°C. Arrows indicate the nuclear localization of ROS formation. (B) ROS formation in A549 cells is observed only with the AKR substrate (B[a]P-7,8-*trans*-dihydrodiol) and the AKR product (B[a]P-7,8-dione). ROS formation is not seen with 20  $\mu$ M B[a]P-4,5-*trans*-dihydrodiol or 20  $\mu$ M *anti*-B[a]PDE under these conditions. (C) Flow cytometric analysis of ROS production in B[a]P metabolite-treated A549 cells. (D) Desferal (1 mM) and 250  $\mu$ M  $\alpha$ -tocopherol attenuate ROS formation-mediated by B[a]P metabolites in A549 cells as measured by FACS. Significant changes in ROS after PAH treatment or PAH treatment plus ROS attenuators were seen (\*\*,  $P < 0.005$ ).

Both B[a]P-7,8-*trans*-dihydrodiol and B[a]P-7,8-dione were consumed so that by 12 h no organic metabolites were detected because of the formation of water-soluble metabolites.

In intact A549 cells, conversion of 10  $\mu$ M B[a]P-7,8-*trans*-dihydrodiol to B[a]P-7,8-dione was observed (Fig. 1D). B[a]P-7,8-*trans*-dihydrodiol was gradually depleted at 12 h, and the concurrent formation of B[a]P-7,8-dione ( $M+H$   $m/z = 283$ ) and B[a]P-tetraol-1 (hydrolyzed product of *anti*-B[a]PDE;  $M+H$   $m/z = 321$ ) was observed, suggesting that P450s were also involved in the metabolic activation of B[a]P-7,8-*trans*-dihydrodiol in A549 cells.

These results agree with our previous work in which 7,12-dimethylbenz[a]anthracene-3,4-dihydrodiol was converted to 7,12-dimethylbenz[a]anthracene-3,4-dione in A549 lung cell extracts (20), and B[a]P-7,8-*trans*-dihydrodiol was converted to B[a]P-7,8-dione in H358 cells stably transfected with AKR1A1 (19).

**Fluorescent Detection of ROS Production in A549 Cells Treated with PAH Metabolites.** We next measured whether PAH metabolites cause ROS formation in intact A549 cells. Using the fluorescent dye dichlorodihydrofluorescein diacetate (DCFH-DA), ROS formation was detected in B[a]P-7,8-*trans*-dihydrodiol-treated (AKR substrate) and B[a]P-7,8-dione (AKR product)-treated A549 cells in a concentration-dependent manner (Fig. 2A). Only the results obtained with 20  $\mu$ M PAH metabolite are presented but increases in fluorescence intensity were observed with concentrations as low as 200–500 nM [supporting information (SI) Fig. S1]. These findings are consistent with the metabolism data, which indicated that B[a]P-7,8-dione was generated in A549 cell extracts treated with B[a]P-7,8-*trans*-dihydrodiol. Use of ROS attenuators, 1 mM desferal, and 250  $\mu$ M  $\alpha$ -tocopherol decreased the ROS signal in B[a]P-7,8-*trans*-dihydrodiol-treated and B[a]P-7,8-dione-treated A549 cells (Fig. 2A), suggesting that the signal was ROS-dependent.

No detectable ROS formation was observed in cells treated with either ( $\pm$ )-*trans*-4,5-dihydroxy-4,5-dihydro B[a]P (B[a]P-

4,5-*trans*-dihydrodiol) (a regioisomer of B[a]P-7,8-*trans*-dihydrodiol and non-AKR substrate; Scheme S1) or *anti*-B[a]PDE (Fig. 2B). In contrast, cells treated with B[a]P-7,8-*trans*-dihydrodiol and B[a]P-7,8-dione produced ROS. These data confirmed that PAH-mediated ROS formation in A549 cells was AKR-dependent.

ROS formation in A549 cells treated with B[a]P-7,8-*trans*-dihydrodiol or B[a]P-7,8-dione was quantified by FACS analysis. The cell distribution pattern (side light scatter vs. forward light scatter) showed no difference between the control and PAH treatment groups (Fig. S2). The percentage of viable cells was maintained at 93% throughout the experiments, showing that there were no cytotoxic effects observed with any PAH treatment. Both B[a]P-7,8-*trans*-dihydrodiol and B[a]P-7,8-dione increased the fluorescent intensity, indicating that ROS were clearly generated (Fig. 2C). The mean fluorescence index of the entire A549 cell population was  $20.9 \pm 1.0$  for B[a]P-7,8-*trans*-dihydrodiol and  $86.3 \pm 6.4$  for B[a]P-7,8-dione, respectively, as compared with  $4.3 \pm 0.5$  for the DCFH-DA control (Fig. 2D). Inclusion of a mixture of ROS attenuators desferal and  $\alpha$ -tocopherol decreased the B[a]P-7,8-*trans*-dihydrodiol-mediated and B[a]P-7,8-dione-mediated fluorescence intensities by >50% and 66%, respectively (Fig. 2D).

**B[a]P-7,8-*trans*-Dihydrodiol and B[a]P-7,8-Dione Decrease the Cellular Redox State of A549 Cells.** Treatment of A549 cells with PAH metabolites resulted in changes in redox state in A549 cells. B[a]P-7,8-*trans*-dihydrodiol, B[a]P-7,8-dione, and 2-methyl-1,4-naphthalenedione (menadione) (20  $\mu$ M) decreased the levels of reduced glutathione (GSH) in A549 cells by 62%, 42%, and 91%, respectively when compared with the DMSO control (Fig. S3A). The amounts of GSH were measured by HPLC-ECD (23), and the assays were validated by spiking with known amounts of the analyte, where recovery was >95%.

Identical treatments with B[a]P-7,8-*trans*-dihydrodiol, B[a]P-7,8-

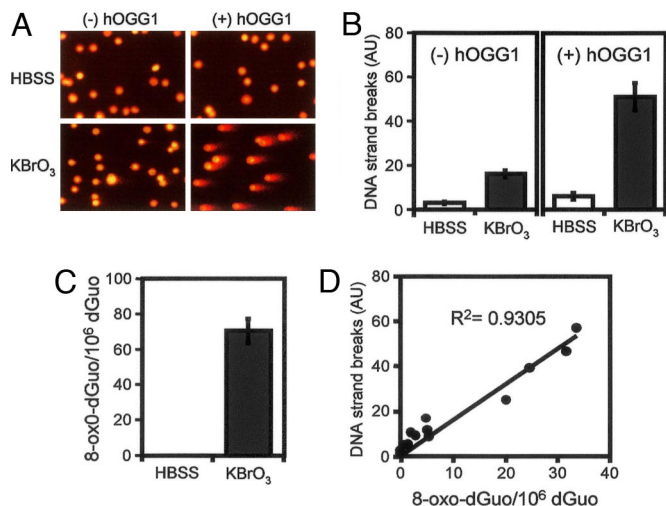


**Fig. 3.** Use of hOGG1-coupled comet assay for detecting 8-oxo-dGuo as strand breaks and its validation by LC-ESI/MS. (A) Typical DNA comet images of KBrO<sub>3</sub> (2.5 mM)-treated A549 cells obtained from single-cell gel electrophoresis assay measured in the presence or absence of hOGG1. (B) Quantification of strand breaks in the presence and absence of hOGG1. (C) Detection of 8-oxo-dGuo measured by LC-ESI/MS in KBrO<sub>3</sub>-treated A549 cells. (D) Correlation between the formation of DNA strand breaks in the hOGG1-coupled comet assay and 8-oxo-dGuo detected by LC-ESI/MS after KBrO<sub>3</sub> treatment. The correlation was observed in H358 cells that were treated with increasing concentrations of KBrO<sub>3</sub> (0.2–1.5 mM) of KBrO<sub>3</sub> for 6 h.

dione, and menadione increased in the intracellular NADP<sup>+</sup>/NADPH ratio in A549 cells. B[a]P-7,8-*trans*-dihydrodiol, B[a]P-7,8-dione, and menadione increased the NADP<sup>+</sup>/NADPH ratio by 3-, 3-, and 8-fold, respectively when compared with the DMSO control (Fig. S3B). The amounts of NADP<sup>+</sup> and NADPH were measured by enzymatic cycling after destruction of the oxidized or reduced pyridine nucleotide (24). The assays were validated by spiking known amounts of the analyte where recovery was >95%. Thus, prolonged exposure with both B[a]P-7,8-*trans*-dihydrodiol and B[a]P-7,8-dione resulted in a prooxidant state in A549 cells.

**The Use of hOGG1-Coupled Comet Assay for Detecting 8-Oxo-dGuo and Its Validation by LC-ESI/MS.** The ability of B[a]P-7,8-*trans*-dihydrodiol to induce 8-oxo-dGuo formation in lung cells is hampered by the difficulty in detecting 8-oxo-dGuo levels reliably in cellular DNA (25). To assess 8-oxo-dGuo levels in cells, the single-cell gel electrophoresis (comet) assay was coupled with hOGG1, which catalyzes the excision of 8-oxo-dGua to yield DNA strand breaks. KBrO<sub>3</sub>, a cellular oxidant that is known to cause 8-oxo-dGuo formation, was used as a positive control (26).

Without hOGG1 treatment, KBrO<sub>3</sub> alone did not induce sufficient levels of DNA strand scission in lung cells when compared with Hanks' buffered salt solution (HBSS) control (Fig. 3A and B). The inclusion of hOGG1 produced significantly more DNA strand breaks in KBrO<sub>3</sub>-treated A549 cells than were observed in its absence (Fig. 3A and B). The detection of 8-oxo-dGuo by the hOGG1-coupled comet assay was validated by using a stable isotope ([<sup>15</sup>N<sub>3</sub>]-8-oxo-dGuo) dilution LC-ESI/multiple reaction monitoring (MRM)/MS assay coupled with immunoaffinity purification to analyze the oxidatively damaged DNA (Fig. 3C). The results show that the coupled assay provides a good estimate for 8-oxo-dGuo present in KBrO<sub>3</sub>-treated A549 cells. Furthermore, when this assay was applied to H358 cells a direct linear correlation between strand breaks and 8-oxo-dGuo observed in the LC-MS assay ( $R^2 = 0.9305$ ) was observed (Fig. 3D). This assay could thus be used to measure the abundance of 8-oxo-dGuo reliably in lung cells treated with B[a]P-7,8-*trans*-dihydrodiol.

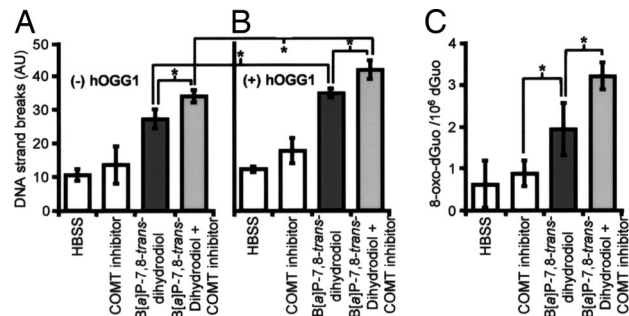


**Fig. 4.** The effects of COMT inhibitor on the formation of DNA strand breaks detected by comet assay in the absence or presence of hOGG1 (A and B) and 8-oxo-dGuo detection by LC-ESI/MS analysis (C) in B[a]P-7,8-*trans*-dihydrodiol-treated A549 cells. Cells were treated with 20 μM B[a]P-7,8-*trans*-dihydrodiol in 3% DMSO in the absence and presence of 3 μM of COMT inhibitor for 6 h. The cells were harvested and divided into two aliquots. One aliquot was used for the detection of DNA strand breaks by the hOGG1-coupled comet assay and the other was used for the detection of 8-oxo-dGuo using immunoaffinity LC-ESI/MS analysis. Significant effects were observed after the hOGG1 and COMT inhibitor treatments (\*,  $P < 0.05$ ; A). Significant effects were observed after treatment with B[a]P-7,8-*trans*-dihydrodiol ± COMT inhibitor (\*,  $P < 0.05$ ).

**Detection of DNA Strand Breaks and 8-Oxo-dGuo in B[a]P-7,8-*trans*-Dihydrodiol-Treated A549 Cells.** To determine whether AKR-dependent conversion of B[a]P-7,8-*trans*-dihydrodiol to B[a]P-7,8-dione in A549 cells increases DNA strand breaks and 8-oxo-dGuo, cells were treated with B[a]P-7,8-*trans*-dihydrodiol in the presence and absence of the catechol *O*-methyl transferase (COMT) inhibitor (2-fluoro-3,4-dihydroxy-5-nitrobenzophenone) for 6 h. B[a]P-7,8-*trans*-dihydrodiol produced more DNA strand breaks in A549 cells when a COMT inhibitor was present and these breaks were increased further by treatment with hOGG1 (Fig. 4A and B).

A similar pattern was observed in the formation of 8-oxo-dGuo in A549 cells when measured by LC-MS. The COMT inhibitor increased the formation of 8-oxo-dGuo in B[a]P-7,8-*trans*-dihydrodiol-treated cells, showing that this lesion was produced by ROS formed during the redox cycling of B[a]P-7,8-dione produced by the AKR pathway (Fig. 4C).

## Discussion

We have demonstrated that the AKR pathway for PAH *trans*-dihydrodiol activation results in ROS formation and a prooxidant cellular state and causes oxidative DNA damage (hOGG1-specific DNA strand breaks and 8-oxo-dGuo) in human lung adenocarcinoma A549 cells.

Our recent metabolism studies showed that the P450 1A1/1B1 and the AKR pathways can effectively compete for B[a]P-7,8-*trans*-dihydrodiol activation in AKR1A1 stably transfected H358 cells (19). In the present work, we exploited A549 cells because they have high constitutive expression of AKR1C1–1C3 isoforms (20). It has also been reported that P450 1A1/1B1 can be induced via the aryl hydrocarbon receptor (AhR) in A549 cells (27), suggesting that these cells could be used to examine both pathways without genetic manipulation. Our metabolism studies using P450 1A1/1B1-uninduced A549 cells support this concept because B[a]P-7,8-*trans*-dihydrodiol is simultaneously converted to B[a]P-tetraols (hydrolysis products of *anti*-B[a]PDE) and B[a]P-7,8-dione. Therefore, these cells provide a unique and useful cell line to compare the metabolic profile of PAH by both P450 and AKRs.

We find that B[a]P-7,8-*trans*-dihydrodiol (AKR substrate) and B[a]P-7,8-dione (AKR product) generate ROS *in situ* in A549 cells pretreated with DCFH-DA, and this effect is suppressed by ROS attenuators (Fig. 2A). Because ROS formation is not

observed in A549 cells treated with either a regioisomer of B[a]P-7,8-*trans*-dihydrodiol (B[a]P-4,5-*trans*-dihydrodiol) or a product of further P450 metabolism (*anti*-B[a]PDE), PAH-metabolite induced ROS formation is solely AKR-dependent (Fig. 2B). The fluorescent signal was also nuclear in localization, indicative of a transport mechanism for B[a]P-7,8-dione (Fig. 2A and B and Fig. S1, arrow). We have reported that this PAH *o*-quinone acts as a ligand for the AhR (28). These findings suggest that ROS-mediated DNA damage by PAH *o*-quinones may depend on transport by the AhR.

Treatment of A549 cells with B[a]P-7,8-*trans*-dihydrodiol or B[a]P-7,8-dione caused a decrease in GSH levels with a concomitant increase in the intracellular NADP<sup>+</sup>/NADPH ratio (Fig. S3). Interestingly, the bolus addition of B[a]P-7,8-dione also caused a decrease in oxidized glutathione, which likely reflects GSH-conjugate formation. The B[a]P-7,8-dione-GSH conjugate is redox-active in its own right (T.M.P., unpublished observation). Thus the changes in the NADP<sup>+</sup>/NADPH ratio are likely associated with PAH metabolite-mediated ROS formation, the elimination of peroxides by the GSH peroxidase system, and depletion of NADPH. Similar changes in redox state have been observed in V79 cells after treatment with *p*-quinones (29).

PAH *o*-quinones produced by AKRs cause oxidative DNA damage in the form of 8-oxo-dGuo *in vitro* (30). However, whether 8-oxo-dGuo could be detected reliably as a result of PAH activation by AKRs in intact cells was unknown. To test this possibility, hOGG1 was coupled to the comet assay technique (26). hOGG1 is a base excision repair enzyme, which excises 8-oxo-Gua from DNA (31). This reaction results in the formation of AP sites that through a  $\beta$ -elimination process subsequently causes overt strand breaks in the DNA. The hOGG1-coupled comet assay made it possible to detect 8-oxo-dGuo as DNA strand breaks in human lung A549 cells after PAH treatment. However, because hOGG1 can recognize 2,6-diamino-4-hydroxy-5-formamidopyrimidine (Fapy-Gua) that can be formed by ROS, caution was required in measuring 8-oxo-dGuo, especially when using the hOGG1-coupled comet assay alone. Our LC-MS data provides confidence that the hOGG1-coupled comet assay is a semiquantitative method to detect 8-oxo-dGuo in lung cells (Fig. 3).

The hOGG1-coupled comet assay showed that B[a]P-7,8-*trans*-dihydrodiol generated overt strand breaks in A549 cell DNA. Furthermore, the fact that the COMT inhibitor amplified B[a]P-7,8-*trans*-dihydrodiol-mediated DNA strand breaks and 8-oxo-dGuo formation in the cellular DNA indicates that these events occur as result of AKR-dependent conversion of B[a]P-7,8-*trans*-dihydrodiol to B[a]P-7,8-dione and its subsequent redox cycling back to the catechol (Fig. 4). These findings suggest that AKR-dependent PAH activation can induce ROS and the ROS formed causes oxidative DNA damage in the form of 8-oxo-dGuo in human lung cells.

Although the formation of covalent PAH-DNA adducts has been extensively studied as a known mechanism for PAH carcinogenesis (2, 3, 6), our study suggests that formation of PAH-mediated oxidative DNA damage may also contribute to carcinogenesis. PAHs have previously been reported to cause oxidative DNA damage *in vitro* and *in vivo* when using methods of varying sensitivity and specificity (32, 33). Base modifications such as thymine glycol, etheno adducts, and 8-oxo-dGuo all have been detected upon PAH exposure (34). However, the mechanism by which PAH can cause oxidative DNA damage has been uncertain. Our results show that AKR-dependent PAH activation can account for the oxidative DNA damage caused by parent PAHs and PAH *trans*-dihydrodiols. In addition, our *in vitro* *p53* mutagenesis studies showed that PAH *o*-quinones produced by AKRs generate 8-oxo-dGuo and cause G-to-T transversions in *p53* cDNA, and that these effects were abolished by ROS scavengers (16, 17), suggesting a

direct relationship between oxidative DNA damage and the observed mutational pattern in *p53*.

Interestingly, the loss of heterozygosity of hOGG1 has been associated with the development of lung cancer (35). Polymorphism in the hOGG1 gene locus and loss of heterozygosity both increase lung cancer susceptibility (36). Patients exhibiting loss of heterozygosity of hOGG1 gene had high levels of 8-oxo-dGuo in their DNA (37). In addition, hOGG1 activity was decreased in peripheral blood monocytes of patients with NSCLC (38), and 8-oxo-dGuo levels were significantly higher in leucocytes of lung cancer patients and healthy smokers when compared with healthy nonsmokers (39). This finding suggests that during lung cancer development, cells may have an increased mutational load because of the inability to repair 8-oxo-dGuo.

Clinical and epidemiological studies support the concept that AKR isoforms, which lead to oxidative DNA damage, can contribute to the initiation of lung cancer (21, 22). Moreover, AKR expression in human oral squamous cell carcinoma has been observed after areca-*quid* chewing in combination with smoking (40). Exposure of human buccal cells to 1-hydroxychavicol (a major ingredient of areca-*quid*) induced AKR1C1, and subsequent treatment with B[a]P caused a decrease in bulky stable adducts as measured by [<sup>32</sup>P]-postlabeling together with a concomitant increase in 8-oxo-dGuo as measured by HPLC-ECD. Unfortunately, the analytical methods used in these studies had questionable specificity.

In summary, our data show that oxidation of B[a]P-7,8-*trans*-dihydrodiol to B[a]P-7,8-dione by AKRs results in ROS generation, a prooxidant cellular state, and oxidative DNA damage in human lung A549 adenocarcinoma cells. These results provide strong evidence that AKR-dependent PAH activation and the resultant ROS formation could contribute to PAH-mediated lung mutagenesis and carcinogenesis.

## Materials and Methods

**PAH Metabolites.** ( $\pm$ )[1,3-<sup>3</sup>H]-B[a]P-7,8-*trans*-dihydrodiol (specific activity 1,170 cpm/nmol,  $\geq$  98% pure by HPLC), ( $\pm$ )B[a]P-7,8-*trans*-dihydrodiol, ( $\pm$ )B[a]P-4,5-*trans*-dihydrodiol, ( $\pm$ )B[a]P-7,8-dione, and ( $\pm$ )*anti*-B[a]PDE were purchased from the National Cancer Institute Chemical Carcinogen Standard Reference Repository (Midwest Research Institute, Kansas City) or synthesized according to published methods (41).

**Cells and PAH Treatment.** A549 human lung adenocarcinoma cells were obtained from the American Type Culture Collection (ATCC no. CCL-185) and cultured as recommended. The cells were treated with PAH metabolites as follows. Ninety to 100% confluent cells were washed with HBSS buffer containing Mg<sup>2+</sup> and Ca<sup>2+</sup> and treated with the same HBSS buffer containing 0–20  $\mu$ M of B[a]P-7,8-*trans*-dihydrodiol, B[a]P-7,8-dione, B[a]P-4,5-*trans*-dihydrodiol, or *anti*-B[a]PDE in 2% DMSO.

**Oxidation of B[a]P-7,8-*trans*-Dihydrodiol to B[a]P-7,8-Dione by AKR1C Isoforms in A549 Cell Extracts and Intact Cells.** Chromatographic analysis, separation, and quantification of PAH metabolites *in vitro* and *in vivo* were achieved as described (18, 19). A detailed description of the PAH metabolism experiments is found in *SI Text*.

**Detection of Intracellular ROS Produced by PAH Metabolites.** Formation of intracellular ROS in PAH-treated A549 cells was measured with DCFH-DA dye. Formation of intracellular ROS was also measured by a fluorescence-activated cell sorter (FACS-calibur; Becton-Dickinson) equipped with an argon laser, yielding a 488-nm primary emission line. Detailed descriptions of these methods can be found in *SI Text*.

**Measurement of Intracellular GSH.** A549 cells ( $1 \times 10^7$  cells) were homogenized in 200 mM methane sulfonic acid containing 5 mM diethylenetriamine pentaacetic acid by sonication. Intracellular GSH was measured in the homogenates by HPLC-ECD assay with an ESA Couarray detector (23). A detailed description of the measurement of reduced GSH can be found in *SI Text*.

**Measurement of Intracellular Reduced and Oxidized Pyridine Nucleotides [NADP(H)].** Intracellular amounts of NADPH and NADP<sup>+</sup> were measured in cell lysates spectrophotometrically after destruction of either the contaminating

oxidized or reduced cofactors, respectively, followed by enzymatic cycling (24). Detailed descriptions for the quantification of the oxidized and reduced pyridine nucleotide cofactors can be found in *SI Text*.

**Measurement of DNA Strand Breaks in PAH-Treated A549 Cells.** DNA strand breaks in PAH-treated A549 cells were measured by using a modified comet assay technique as described (26). Detailed descriptions of this assay and the quantification of DNA strand breaks can be found in *SI Text*.

**Quantification of 8-Oxo-dGuo by LC-ESI/MRM/MS in PAH-Treated A549 Cells.** Genomic DNA was extracted from PAH-treated cells by using DNAzol BD

(Invitrogen). The DNA was quantitatively digested by the addition of DNase I, phosphodiesterase I (from *Crotalus adamanteus* venom), and shrimp alkaline phosphatase and spiked with an internal standard [<sup>15</sup>N<sub>5</sub>]-8-oxo-dGuo. The DNA samples were divided into two aliquots. One aliquot was used for the isolation and quantification of 8-oxo-dGuo via immunoaffinity purification stable isotope dilution LC-MRM/MS analysis. The other aliquot was used for DNA base analysis. Detailed descriptions of 8-oxo-dGuo detection and base analysis can be found in *SI Text*.

**ACKNOWLEDGMENTS.** This work was supported by National Institutes of Health Grants R01CA-39504, R01ES015857, and P30ES013508 (to T.M.P.) and R25CA101871 and R01CA130038 (to I.A.B.).

- Grimmer G, Bohnke H (1975) Polycyclic aromatic hydrocarbon profile analysis of high-protein foods, oils, and fats by gas chromatography. *J Assoc Off Anal Chem* 58:725–733.
- Xue W, Warshawsky D (2005) Metabolic activation of polycyclic and heterocyclic aromatic hydrocarbons and DNA damage: A review. *Toxicol Appl Pharmacol* 206:73–93.
- Hecht SS (1999) Tobacco smoke carcinogens and lung cancer. *J Natl Cancer Inst* 91:1194–1210.
- Marshall CJ, Vousden KH, Phillips DH (1984) Activation of c-Ha-ras-1 protooncogene by *in vitro* modification with a chemical carcinogen, benzo(a)pyrene diol-epoxide. *Nature* 310:586–589.
- Denissenko MF, Pao A, Tang M, Pfeifer GP (1996) Preferential formation of benzo[a]pyrene adducts at lung cancer mutational hotspots in P53. *Science* 274:430–432.
- Conney AH (1982) Induction of microsomal enzymes by foreign chemicals and carcinogenesis by polycyclic aromatic hydrocarbons: G. H. A. Clowes Memorial Lecture. *Cancer Res* 42:4875–4917.
- Zhang Y, et al. (2000) Error-prone lesion bypass by human DNA polymerase  $\epsilon$ . *Nucleic Acids Res* 28:4717–4724.
- Cavaliere EL, Rogan EG (1995) Central role of radical cations in metabolic activation of polycyclic aromatic hydrocarbons. *Xenobiotica* 25:677–688.
- Sagher D, Strauss B (1985) Abasic sites from cytosine as termination signals for DNA synthesis. *Nucleic Acids Res* 13:4285–4298.
- Penning TM, et al. (1999) Dihydrodiol dehydrogenases and polycyclic aromatic hydrocarbon activation: Generation of reactive and redox active o-quinones. *Chem Res Toxicol* 12:1–18.
- Balu N, et al. (2004) Identification and characterization of novel stable deoxyguanosine and deoxyadenosine adducts of benzo[a]pyrene-7,8-quinone from reactions at physiological pH. *Chem Res Toxicol* 17:827–838.
- McCoull KD, Rindgen D, Blair IA, Penning TM (1999) Synthesis and characterization of polycyclic aromatic hydrocarbon o-quinone depurinating N7-guanine adducts. *Chem Res Toxicol* 12:237–246.
- Cerutti PA (1985) Prooxidant states and tumor promotion. *Science* 227:375–381.
- Cheng KC, et al. (1992) 8-Hydroxyguanine, an abundant form of oxidative DNA damage, causes G-T and A-C substitutions. *J Biol Chem* 267:166–172.
- Bolton JL, et al. (2000) Role of quinones in toxicology. *Chem Res Toxicol* 13:135–160.
- Yu D, Berlin JA, Penning TM, Field J (2002) Reactive oxygen species generated by PAH o-quinones cause change-in-function mutations in p53. *Chem Res Toxicol* 15:832–842.
- Park J-H, et al. (2008) The pattern of P53 mutation caused by PAH o-quinones is driven by 8-oxo-dGuo formation while the spectrum of mutations is determined by biological selection for dominance. *Chem Res Toxicol* 21, in press.
- Jiang H, Shen YM, Quinn AM, Penning TM (2005) Competing roles of cytochrome P450 1A1/1B1 and aldo-keto reductase 1A1 in the metabolic activation of (+/-)-7,8-dihydroxy-7,8-dihydro-benzopyrene in human bronchoalveolar cell extracts. *Chem Res Toxicol* 18:365–374.
- Jiang H, Vudathala DK, Blair IA, Penning TM (2006) Competing roles of aldo-keto reductase 1A1 and cytochrome P4501B1 in benzo[a]pyrene-7,8-diol activation in human bronchoalveolar H358 cells: Role of AKRs in P4501B1 induction. *Chem Res Toxicol* 19:68–78.
- Palackal NT, et al. (2002) Activation of polycyclic aromatic hydrocarbon trans-dihydrodiol proximate carcinogens by human aldo-keto reductase (AKR1C) enzymes and their functional overexpression in human lung carcinoma (A549) cells. *J Biol Chem* 277:24799–24808.
- Woenckhaus M, et al. (2006) Smoking and cancer-related gene expression in bronchial epithelium and non-small-cell lung cancers. *J Pathol* 210:192–204.
- Fukumoto S, et al. (2005) Overexpression of the aldo-keto reductase family protein AKR1B10 is highly correlated with smokers' non-small cell lung carcinomas. *Clin Cancer Res* 11:1776–1785.
- Lakritz J, Plopper CG, Buckpitt AR (1997) Validated high-performance liquid chromatography-electrochemical method for determination of glutathione and glutathione disulfide in small tissue samples. *Anal Biochem* 247:63–68.
- Lowry OH, Passoneau JV, Rock MK (1961) The measurement of pyridine nucleotides by enzymatic cycling. *J Biol Chem* 236:2756–2759.
- European Standards Committee on Oxidative DNA Damage, Gedik CM, Collins A (2005) Establishing the background level of base oxidation in human lymphocyte DNA: Results of an interlaboratory validation study. *FASEB J* 19:82–84.
- Smith CC, O'Donovan MR, Martin EA (2006) hOGG1 recognizes oxidative damage using the comet assay with greater specificity than FPG or ENDOIII. *Mutagenesis* 21:185–190.
- Foster KA, et al. (1998) Characterization of the A549 cell line as a type II pulmonary epithelial cell model for drug metabolism. *Exp Cell Res* 243:359–366.
- Burczynski ME, Penning TM (2000) Genotoxic polycyclic aromatic hydrocarbon ortho-quinones generated by aldo-keto reductases induce CYP1A1 via nuclear translocation of the aryl hydrocarbon receptor. *Cancer Res* 60:908–915.
- Ludewig G, Dogra S, Glatt H (1989) Genotoxicity of 1,4-benzoquinone and 1,4-naphthoquinone in relation to effects on glutathione and NAD(P)H levels in V79 cells. *Environ Health Perspect* 82:223–228.
- Park J-H, et al. (2005) Formation of 8-oxo-7,8-dihydro-2'-deoxyguanosine (8-oxo-dGuo) by PAH o-quinones: Involvement of reactive oxygen species and copper(II)/copper(I) redox cycling. *Chem Res Toxicol* 18:1026–1037.
- Björås M, et al. (1997) Opposite base-dependent reactions of a human base excision repair enzyme on DNA containing 7,8-dihydro-8-oxoguanine and abasic sites. *EMBO J* 16:6314–6322.
- Leadon SA, Stampfer MR, Bartley J (1988) Production of oxidative DNA damage during the metabolic activation of benzo[a]pyrene in human mammary epithelial cells correlates with cell killing. *Proc Natl Acad Sci USA* 85:4365–4368.
- Leadon SA, Sumerel J, Minton TA, Tischler A (1995) Coal tar residues produce both DNA adducts and oxidative DNA damage in human mammary epithelial cells. *Carcinogenesis* 16:3021–3026.
- Kim KB, Lee BM (1997) Oxidative stress to DNA, protein, and antioxidant enzymes (superoxide dismutase and catalase) in rats treated with benzo(a)pyrene. *Cancer Lett* 113:205–212.
- Chevillard S, et al. (1998) Mutations in OGG1, a gene involved in the repair of oxidative DNA damage, are found in human lung and kidney tumors. *Oncogene* 16:3083–3086.
- Wikman H, et al. (2000) hOGG1 polymorphism and loss of heterozygosity (LOH): Significance for lung cancer susceptibility in a Caucasian population. *Int J Cancer* 88:932–937.
- Hardie LJ, et al. (2000) The effect of hOGG1 and glutathione peroxidase I genotypes and 3p chromosomal loss on 8-hydroxydeoxyguanosine levels in lung cancer. *Carcinogenesis* 21:167–172.
- Paz-Elizur T, et al. (2003) DNA repair activity for oxidative damage and risk of lung cancer. *J Natl Cancer Inst* 95:1312–1319.
- Gackowski D, et al. (2003) Products of oxidative DNA damage and repair as possible biomarkers of susceptibility to lung cancer. *Cancer Res* 63:4899–4902.
- Tang DW, Chang KW, Chi CW, Liu TY (2004) Hydroxychavicol modulates benzo[a]pyrene-induced genotoxicity through induction of dihydrodiol dehydrogenase. *Toxicol Lett* 152:235–243.
- Harvey RG, Dai Q, Ran C, Penning TM (2004) Synthesis of the o-quinones and other oxidized metabolites of polycyclic aromatic hydrocarbons implicated in carcinogenesis. *J Org Chem* 69:2024–2032.